

Bell inequality violation and operator ordering in quantum theoryH. M. Faria, K. Dechoum , and A. Z. Khoury *Instituto de Física, Universidade Federal Fluminense, 24210-346 Niterói, RJ, Brasil*

(Received 12 April 2020; accepted 29 October 2020; published 13 November 2020)

We investigate the role played by quantum operator ordering in the correlations that characterize two-photon polarization Bell measurements. The Clauser-Horne-Shimony-Holt (CHSH) criterion is investigated in the normal ordering imposed by the photodetection theory and in the symmetric ordering that constitutes the standard prescription for building Hermitian operators from products of noncommuting observables. The two approaches are obtained in a single theoretical framework, where operator ordering is directly associated with the representation used for the density matrix. Moreover, this discussion can be recast in terms of the contribution given by the vacuum fluctuations to the detected signals. We also envisage possible detection schemes sensitive to these fluctuations with recent technological developments.

DOI: [10.1103/PhysRevA.102.053714](https://doi.org/10.1103/PhysRevA.102.053714)**I. INTRODUCTION**

Bell inequality violation has been used as a key criterion for identifying nonlocal or noncontextual correlations in quantum mechanics [1–16]. It is one of the pillars that distinguish quantum from classical correlations and also plays a major role in quantum information protocols. Since the seminal experiment by Aspect and co-workers [2], many different tests of the Clauser-Horne-Shimony-Holt (CHSH) inequality [17] have been performed with entangled photon pairs. These photonic tests of the CHSH criterion rely on intensity correlations measured with photodetectors, which are subject to the assumptions adopted in the realm of photodetection theory [18]. For example, intensity correlations are given by normally ordered correlation functions of the electromagnetic field operators. This normal ordering stems from the destructive nature of the detection mechanism through photon absorption. It also prevents any influence from the quantum vacuum, since its energy cannot be extracted by the photodetectors. In this sense, Bell's inequality violation can be affected by a vacuum sensitive detection system.

Nevertheless, symmetric ordering is the prescription for constructing Hermitian operators composed by products of noncommuting observables. In this context, phase-space quantum distributions play a key role in calculating averages, such as correlation functions, in a given operator ordering. For example, the Glauber P-distribution is associated with averages of normally ordered operator products, while the Wigner distribution corresponds to averages in symmetric ordering [19]. Beyond a simple technical issue, this operator ordering has a more profound meaning regarding the vacuum contribution to intensity correlation measurements in quantum optical experiments. This is a long standing concern and we may quote an interesting discussion presented in Ref. [20] about the role played by operator ordering in correctly accounting for the contribution of vacuum fluctuations in radiation reaction. More recently, operator ordering sensitivity has been related to the nonclassicality of bosonic field quantum states [21].

As we mentioned, photodetection signals naturally give normally ordered intensity correlations with vanishing vacuum contribution. Interestingly, the symmetrically ordered intensity correlations given by the Wigner representation encompass vacuum fluctuations and coincides with the results given by a classical stochastic model for the background noise [22]. Such classical models have already been used to describe optical phenomena related to the vacuum fluctuations [22–25]. Moreover, the quantum-classical boundary has been recently revisited in a number of research works with the aid of new theoretical tools for characterizing polarization in different optical degrees of freedom and the corresponding correlations [26–31].

This paper aims to investigate the role played by operator ordering in Bell inequality violation with polarization entangled photons. We compare different ordering choices in the intensity correlations that figure in the CHSH inequality. We show that violation is precluded by symmetric ordering, which means that the *blindness* of the photodetectors to the quantum vacuum plays an important role.

II. QUANTUM DESCRIPTION OF PARAMETRIC DOWN CONVERSION

Let us apply our ideas to a frequently used source of polarization entangled photon pairs [32–34]. It is composed of two identical nonlinear crystals glued together with their optical axes rotated by 90° relative to each other. A strong laser beam at frequency ω is used to pump the crystals and generate photon pairs at frequency $\omega/2$ by spontaneous parametric down conversion (SPDC). The pump beam is linearly polarized at 45° with respect to the crystals axes. Under type-I phase match, a pair of linearly polarized photons is generated either with horizontal polarization in one crystal or with vertical polarization in the other, thus producing a polarization entangled state. Two polarizers are used in the detection region, one before each photodetector, to set the measurement bases. This setup is depicted in Fig. 1. This will be our model

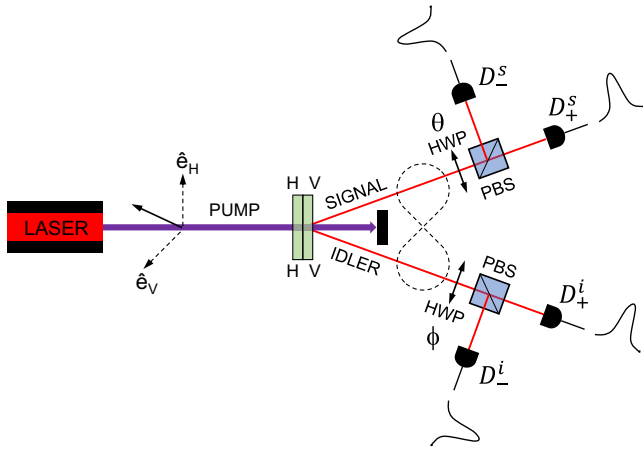


FIG. 1. Typical setup for Bell inequality measurements with a polarization entangled photon source. Two nonlinear crystals are glued together with their optical axes rotated with respect to each other. A pump beam polarized at 45° can generate either horizontally polarized photons in the first crystal or vertically polarized photons in the second. Two-photon polarization analysis is performed in the detection region. Half-wave plates (HWP) are used to set the measurement angles θ and ϕ . Polarization projection is performed with polarizing beam splitters (PBS) before the photons hit detectors D_{\pm}^s and D_{\pm}^i . When measuring symmetrically ordered intensity correlations, these detectors must be replaced by homodyne detection setups.

system for investigating the CHSH inequality under different correlation ordering and the role played by quantum vacuum. For symmetrically ordered intensity correlations, detectors D_{\pm}^s and D_{\pm}^i must be replaced by homodyne detection setups, as will be explained in Sec. V.

For a thin crystal and low nonlinear susceptibility χ , the pump laser is very little affected by the down-conversion process and only a small fraction of the incoming photons is converted into photon pairs. In this case, we can assume that the input quantum state of the pump beam remains unaltered by the parametric interaction. Moreover, we will consider the pump laser polarized at 45° , prepared in a coherent state $|v_p\rangle_H \otimes |v_p\rangle_V$. The Hamiltonians for the SPDC process in crystals 1 and 2 are

$$\begin{aligned}\hat{H}_1 &= i\hbar g \hat{a}_H^{s\dagger} \hat{a}_H^{i\dagger} + \text{H.c.}, \\ \hat{H}_2 &= i\hbar g \hat{a}_V^{s\dagger} \hat{a}_V^{i\dagger} + \text{H.c.},\end{aligned}\quad (1)$$

where $g = \chi v_p$ is the nonlinear coupling constant, \hat{a}_j^s, \hat{a}_j^i ($j = H, V$) are boson operators for signal and idler modes with horizontal (H) and vertical (V) polarizations, and H.c. stands for Hermitian conjugate.

In either Glauber or Wigner representation, the density matrix $\hat{\rho}$ is represented by a quasiprobability distribution $P(\mathbf{a}, \mathbf{a}^*)$ (Glauber) or $W(\mathbf{a}, \mathbf{a}^*)$ (Wigner) for a column vector of complex stochastic amplitudes $\mathbf{a} = (a_H^s, a_V^s, a_H^i, a_V^i)^T$. These distributions are readily obtained from the density matrix through the corresponding characteristic function. The Glauber representation is given as the Fourier transform of

the normally ordered characteristic function C_P [19],

$$\begin{aligned}P(\mathbf{a}, \mathbf{a}^*) &= \frac{1}{\pi^2} \int C_P(\mathbf{z}, \mathbf{z}^*) e^{-i(\mathbf{z}^* \mathbf{a}^* + \mathbf{z} \mathbf{a})} d^2 \mathbf{z}, \\ C_P(\mathbf{z}, \mathbf{z}^*) &= \text{Tr}[\hat{\rho} e^{i(\mathbf{z}^* \hat{\mathbf{a}}^\dagger)} e^{i(\mathbf{z} \hat{\mathbf{a}})}],\end{aligned}\quad (2)$$

where $\mathbf{z} = (z_H^s, z_V^s, z_H^i, z_V^i)$ is a row vector of Fourier variables, one for each mode amplitude, and $\hat{\mathbf{a}} = (\hat{a}_H^s, \hat{a}_V^s, \hat{a}_H^i, \hat{a}_V^i)^T$ is a column vector with the corresponding annihilation operators. Averages of normally ordered operator products for any mode j are readily calculated with the Glauber distribution as follows:

$$\langle \hat{a}_j^{m\dagger} \hat{a}_j^n \rangle_N = \int P(\mathbf{a}, \mathbf{a}^*) a_j^{m*} a_j^n d^2 \mathbf{a}.\quad (3)$$

The Wigner representation is given as the Fourier transform of the symmetrically ordered characteristic function C_W [19],

$$\begin{aligned}W(\mathbf{a}, \mathbf{a}^*) &= \frac{1}{\pi^2} \int C_W(\mathbf{z}, \mathbf{z}^*) e^{-i(\mathbf{z}^* \mathbf{a}^* + \mathbf{z} \mathbf{a})} d^2 \mathbf{z}, \\ C_W(\mathbf{z}, \mathbf{z}^*) &= \text{Tr}[\hat{\rho} e^{i(\mathbf{z}^* \hat{\mathbf{a}}^\dagger + \mathbf{z} \hat{\mathbf{a}})}].\end{aligned}\quad (4)$$

Averages of symmetrically ordered operator products for any mode j are readily calculated with the Wigner distribution as follows:

$$\langle \hat{a}_j^{m\dagger} \hat{a}_j^n \rangle_S = \int W(\mathbf{a}, \mathbf{a}^*) a_j^{m*} a_j^n d^2 \mathbf{a}.\quad (5)$$

For the Hamiltonians given in Eqs. (1), the dynamics of SPDC can be described by a Fokker-Planck equation for the time evolution of both Glauber and Wigner distributions [35–37]. From the corresponding Fokker-Planck equation for P or W , one can derive a set of Langevin equations for the stochastic amplitudes \mathbf{a} . Neglecting losses in the thin crystal regime, these equations are

$$\begin{aligned}\dot{a}_H^s &= g a_H^{i*}, & \dot{a}_V^s &= g a_V^{i*}, \\ \dot{a}_H^i &= g a_H^{s*}, & \dot{a}_V^i &= g a_V^{s*},\end{aligned}\quad (6)$$

where the equations on the left are for crystal 1 and those on the right are for crystal 2. The main difference between the two representations consists of the correlation functions between the input amplitudes, as we will make explicit shortly.

The pump- and down-converted electric fields will be described by plane waves of the form

$$\begin{aligned}\mathbf{E}_p(\mathbf{r}, t) &= v_p (\hat{\mathbf{e}}_H + \hat{\mathbf{e}}_V) e^{i(\mathbf{k}_p \cdot \mathbf{r} - \omega_p t)}, \\ \mathbf{E}_s(\mathbf{r}, t) &= (a_H^s \hat{\mathbf{e}}_H + a_V^s \hat{\mathbf{e}}_V) e^{i(\mathbf{k}_s \cdot \mathbf{r} - \omega_s t)}, \\ \mathbf{E}_i(\mathbf{r}, t) &= (a_H^i \hat{\mathbf{e}}_H + a_V^i \hat{\mathbf{e}}_V) e^{i(\mathbf{k}_i \cdot \mathbf{r} - \omega_i t)},\end{aligned}\quad (7)$$

where \mathbf{k}_j ($j = p, s, i$) is the wave vector of the corresponding mode. We will assume perfect phase match between pump- and down-converted fields, so that $\mathbf{k}_p = \mathbf{k}_s + \mathbf{k}_i$. The input down-converted fields, signal and idler, are assumed to be in vacuum state and the initial values of their amplitudes are complex, Gaussian-distributed stochastic variables that simulate the incoming vacuum fluctuations. These amplitudes obey the following

correlations:

$$\begin{aligned} \langle a_{0k}^j \rangle &= 0, \\ \langle a_{0k}^j a_{0k}^{j'} \rangle &= 0, \\ \langle a_{0k}^j a_{0k'}^{j'*} \rangle &= \frac{\epsilon}{2} \delta_{jj'} \delta_{kk'}, \end{aligned} \quad (8)$$

where $j, j' = s, i$; $k, k' = H, V$, and $\epsilon = 0$ (1) for Glauber (Wigner) representation.

We next solve the dynamical equations for the signal and idler complex amplitudes after passage through both crystals.

A. First crystal

The first crystal converts a vertically polarized pump photon into a pair of horizontally polarized signal and idler photons. The interaction time is $\tau = nd/c$, where d is the propagation distance inside the crystal, n is the refractive index, and c is the speed of light in vacuum. The output complex amplitudes are given by the solution of the left Eqs. (6):

$$\begin{aligned} a_H^s(\tau) &= a_{0H}^s \cosh g\tau + a_{0H}^{i*} \sinh g\tau, \\ a_H^i(\tau) &= a_{0H}^i \cosh g\tau + a_{0H}^{s*} \sinh g\tau. \end{aligned} \quad (9)$$

Note that after passing the first crystal, the signal and idler amplitudes a_H^s and a_H^i exhibit a cross talk between their incoming vacuum fluctuations. This is crucial for understanding the origin of the correlations (entanglement) between signal and idler as a vacuum induced effect. Using the input correlations given in Eq. (8), the output correlations after interaction in the first crystal are

$$\begin{aligned} \langle a_H^j(\tau) \rangle &= 0, \\ \langle a_H^{j*}(\tau) a_H^{j'}(\tau) \rangle &= \left(\frac{\epsilon}{2} + \sinh^2 g\tau \right) \delta_{jj'}, \\ \langle a_H^s(\tau) a_H^i(\tau) \rangle &= \cosh g\tau \sinh g\tau, \end{aligned} \quad (10)$$

where $j, j' = s, i$.

B. Second crystal

The second crystal converts a horizontally polarized pump photon into a pair of vertically polarized signal and idler photons. The interaction time is also τ if we assume the crystals have the same width. The output complex amplitudes are given by the solution of the right Eqs. (6):

$$\begin{aligned} a_V^s(\tau) &= a_{0V}^s \cosh g\tau + a_{0V}^{i*} \sinh g\tau, \\ a_V^i(\tau) &= a_{0V}^i \cosh g\tau + a_{0V}^{s*} \sinh g\tau. \end{aligned} \quad (11)$$

After passing the second crystal, the signal and idler amplitudes a_V^s and a_V^i also exhibit a cross talk between their incoming vacuum fluctuations, inducing correlations (entanglement). Using the input correlations given in Eq. (8), the output correlations after interaction in the second crystal are

$$\begin{aligned} \langle a_V^j(\tau) \rangle &= 0, \\ \langle a_V^{j*}(\tau) a_V^{j'}(\tau) \rangle &= \left(\frac{\epsilon}{2} + \sinh^2 g\tau \right) \delta_{jj'}, \\ \langle a_V^s(\tau) a_V^i(\tau) \rangle &= \cosh g\tau \sinh g\tau, \end{aligned} \quad (12)$$

where $j, j' = s, i$.

C. Polarization measurement settings

After leaving the crystals, the entangled photons travel to the detectors region and traverse two polarizing beam splitters (PBS) preceded by half-wave plates that set the measurement angles at θ (signal) and ϕ (idler) before hitting the detectors. After passing the respective HWP and PBS, each beam will be divided into two polarization components that mix the input H and V amplitudes, producing the following rotated variables:

$$\begin{aligned} a_+^s(\theta) &= a_H^s \cos \theta + a_V^s \sin \theta, \\ a_-^s(\theta) &= a_V^s \cos \theta - a_H^s \sin \theta, \end{aligned} \quad (13)$$

$$\begin{aligned} a_+^i(\phi) &= a_H^i \cos \phi + a_V^i \sin \phi, \\ a_-^i(\phi) &= a_V^i \cos \phi - a_H^i \sin \phi. \end{aligned} \quad (14)$$

The electric field at detectors D_{\pm}^s and D_{\pm}^i will be given by

$$\begin{aligned} E_s(\mathbf{r}_+^s, t) &= a_+^s(\theta) e^{i(\mathbf{k}_s \cdot \mathbf{r}_+^s - \omega_s t)}, \\ E_s(\mathbf{r}_-^s, t) &= a_-^s(\theta) e^{i(\mathbf{k}_s \cdot \mathbf{r}_-^s - \omega_s t)}, \\ E_i(\mathbf{r}_+^i, t) &= a_+^i(\phi) e^{i(\mathbf{k}_i \cdot \mathbf{r}_+^i - \omega_i t)}, \\ E_i(\mathbf{r}_-^i, t) &= a_-^i(\phi) e^{i(\mathbf{k}_i \cdot \mathbf{r}_-^i - \omega_i t)}. \end{aligned} \quad (15)$$

These rotated amplitudes will determine the polarization correlations that figure in the CHSH inequality.

III. FIELD CORRELATIONS

The CHSH criterion for Bell violation is evaluated from coincidence measurements that correspond to intensity correlations between signal and idler. We now calculate several correlation functions in the Glauber and Wigner representations.

A. Individual intensities

First, we calculate the field intensity at each detector

$$\begin{aligned} \langle I_{\pm}^s(\theta) \rangle &= \langle E_s^*(\mathbf{r}_{\pm}^s) E_s(\mathbf{r}_{\pm}^s) \rangle = \langle a_{\pm}^{s*}(\theta) a_{\pm}^s(\theta) \rangle, \\ \langle I_{\pm}^i(\phi) \rangle &= \langle E_i^*(\mathbf{r}_{\pm}^i) E_i(\mathbf{r}_{\pm}^i) \rangle = \langle a_{\pm}^{i*}(\phi) a_{\pm}^i(\phi) \rangle, \end{aligned} \quad (16)$$

Substituting expressions Eqs. (13) and (14), and using the amplitudes correlations given by Eqs. (10) and (11), we arrive at

$$\langle I_{\pm}^s(\theta) \rangle = \langle I_{\pm}^i(\phi) \rangle = \frac{\epsilon}{2} + \sinh^2 g\tau. \quad (17)$$

Note that the individual intensities are insensitive to the polarizers settings. This will be different for the intensity correlations as we show next.

B. Intensity correlations

The input quantum fluctuations on signal and idler fields are uncorrelated before entering the crystals. However, after undergoing parametric interaction within the crystals, their amplitudes become correlated according to Eqs. (10) and (11). The intensity correlations measured on two separate detectors

are given by

$$\begin{aligned} C_{jk}(\theta, \phi) &= \langle E_s^*(\mathbf{r}_j^s) E_s(\mathbf{r}_j^s) E_i^*(\mathbf{r}_k^i) E_i(\mathbf{r}_k^i) \rangle \\ &= \langle I_j^s(\theta) I_k^i(\phi) \rangle, \end{aligned} \quad (18)$$

where $j = \pm$ and $k = \pm$. These intensity correlations can be calculated by using the following relationship that holds for stochastic Gaussian variables:

$$\begin{aligned} \langle a_1 a_2 a_3 a_4 \rangle &= \langle a_1 a_2 \rangle \langle a_3 a_4 \rangle + \langle a_1 a_3 \rangle \langle a_2 a_4 \rangle \\ &\quad + \langle a_1 a_4 \rangle \langle a_2 a_3 \rangle. \end{aligned} \quad (19)$$

With the aid of relation (19), the two-photon polarization correlations can be written as

$$\begin{aligned} C_{jk}(\theta, \phi) &= \langle a_j^{s*}(\theta) a_j^s(\theta) \rangle \langle a_k^{i*}(\phi) a_k^i(\phi) \rangle \\ &\quad + \langle a_j^{s*}(\theta) a_k^{i*}(\phi) \rangle \langle a_j^s(\theta) a_k^i(\phi) \rangle \\ &\quad + \langle a_j^{s*}(\theta) a_k^i(\phi) \rangle \langle a_j^s(\theta) a_k^{i*}(\phi) \rangle. \end{aligned} \quad (20)$$

Using now the correlations given by Eqs. (10) and (12), we find

$$\begin{aligned} C_{++}(\theta, \phi) &= C_{--}(\theta, \phi) \\ &= \frac{(\frac{\epsilon}{2} + \sinh^2 g\tau)^2 + \sinh^2 2g\tau \cos^2(\theta - \phi)}{4}, \end{aligned} \quad (21)$$

$$\begin{aligned} C_{+-}(\theta, \phi) &= C_{-+}(\theta, \phi) \\ &= \frac{(\frac{\epsilon}{2} + \sinh^2 g\tau)^2 + \sinh^2 2g\tau \sin^2(\theta - \phi)}{4}. \end{aligned} \quad (22)$$

We next evaluate the impact of operator ordering on the CHSH criterion for the quantum-classical correlation boundary.

IV. BELL INEQUALITY

Let us apply the Clauser-Horne-Shimony-Holt (CHSH) inequality to the two-photon polarization correlations and compare the results obtained with the symmetric and normal operator ordering. The correlations obtained at a given measurement setting with angles θ (signal) and ϕ (idler) are given by

$$M(\theta, \phi) = \frac{C_{++} + C_{--} - C_{+-} - C_{-+}}{C_{++} + C_{--} + C_{+-} + C_{-+}}. \quad (23)$$

Then, the CHSH inequality is evaluated for the quantity

$$S = M(\theta, \phi) + M(\theta', \phi) - M(\theta, \phi') + M(\theta', \phi'). \quad (24)$$

Classical correlations are restricted to $-2 \leq S \leq 2$. However, this inequality can be violated for quantum correlated polarization modes, where maximum violation occurs when $S = 2\sqrt{2}$. This can be accomplished with the following polarization settings: $\theta = 0$, $\theta' = \pi/4$, $\phi = \pi/8$, and $\phi' = 3\pi/8$, for example. We next check the CHSH inequality in each operator ordering by plugging (21) and (22) into (23) and (24). Note that the ordering dependent terms in Eqs. (21) and (22) cancel out in the numerator of (23) but they do contribute

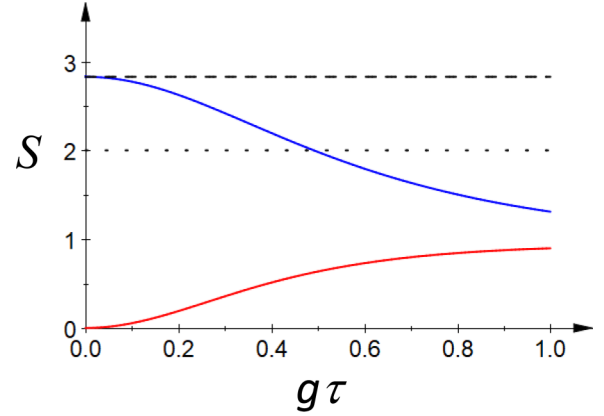


FIG. 2. Bell parameter S for normal (blue) and symmetric (red) ordering. The dashed and dotted lines show the $2\sqrt{2}$ limit and the violation boundary, respectively.

to the denominator. As we show below, it drastically affects the violation of the CHSH criterion in the thin crystal limit $g\tau \ll 1$, usually valid in actual experimental conditions.

(1) Normal ordering

$$\begin{aligned} M(\theta, \phi) &= \left(\frac{\sinh^2 2g\tau}{\sinh^2 2g\tau + 8 \sinh^4 g\tau} \right) \cos[2(\theta - \phi)], \\ S_N &= 2\sqrt{2} \left(\frac{\sinh^2 2g\tau}{\sinh^2 2g\tau + 8 \sinh^4 g\tau} \right) \approx 2\sqrt{2}. \end{aligned} \quad (25)$$

(2) Symmetric ordering

$$\begin{aligned} M(\theta, \phi) &= \left(\frac{\sinh^2 2g\tau}{\sinh^2 2g\tau + 2 \cosh^2 2g\tau} \right) \cos[2(\theta - \phi)], \\ S_S &= 2\sqrt{2} \left(\frac{\sinh^2 2g\tau}{\sinh^2 2g\tau + 2 \cosh^2 2g\tau} \right) \approx 0. \end{aligned} \quad (26)$$

As we can see, in the thin crystal limit ($g\tau \ll 1$) the normally ordered polarization correlations give maximal violation of the CHSH inequality, while the symmetric ordered polarization correlations do not violate. This can be easily visualized in the graphic shown in Fig. 2, where the CHSH quantity S given by Eqs. (25) and (26) is plotted as a function of $g\tau$.

V. MEASUREMENT SCHEME

A natural question to be asked is whether the intensity correlations between the vacuum modes predicted in the symmetric order can be accessed by some mechanism. Let us recall that symmetric ordering is the quantum theory prescription when calculating averages of physical quantities composed by functions of noncommuting observables. This is the case, for example, of the intensity

$$I = X^2 + Y^2 = \frac{aa^\dagger + a^\dagger a}{2}, \quad (27)$$

where we defined the quadratures

$$X = \frac{a + a^\dagger}{2}, \quad Y = \frac{a - a^\dagger}{2i}. \quad (28)$$

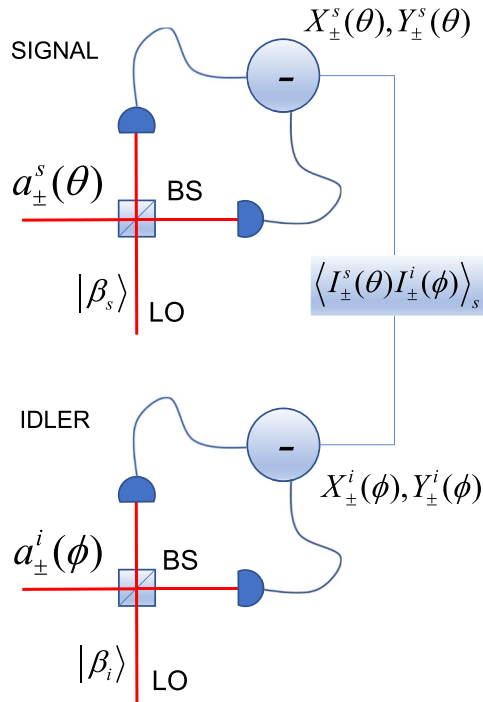


FIG. 3. Measurement scheme for symmetrically ordered correlations. BS: beam splitter, LO: local oscillator.

This quantity is not the one measured in the standard photodetection scheme, which, being based on photon absorption, is not sensitive to antinormal terms. Therefore, the usual schemes have limited access to the field fluctuations, since they are blind to the vacuum field contribution. In order to obtain full information about the field properties by measuring the symmetrically ordered correlation functions, one must perform a direct measurement of the field amplitudes, more precisely the field quadratures. In the radio frequency range of the electromagnetic spectrum, the response of a regular antenna is indeed proportional to the field amplitude and the quadratures can be directly measured. However, discretization of the energy exchange in this regime is negligible and quantum effects cannot be sensed. Meanwhile, direct detection of the fast field oscillations in the optical regime is challenging and one must resort to homodyne measurements. An interesting discussion on experimental techniques for measuring correlation functions in normal, symmetric, and antinormal ordering is presented in Refs. [38,39], where a direct correspondence between operator ordering and detection schemes is summarized as follows:

- (1) normal ordering $a^\dagger a$: direct detection.
- (2) symmetric ordering $(a^\dagger a + a a^\dagger)/2$: homodyne detection.
- (3) antinormal ordering $a a^\dagger$: heterodyne detection.

In the heterodyne (double-homodyne) detection scheme, it is possible to simultaneously measure canonical conjugate quadratures, at the expense of allowing extra (vacuum) noise into the detection mechanism.

The symmetrically ordered averages can be accessed with the homodyne measurement setup depicted in Fig. 3. Each

polarization output of signal and idler is sent to a homodyne detection setup, where it is mixed with a local oscillator prepared in a coherent state $|\beta_j\rangle$ ($j = s, i$). By adjusting the phase of each local oscillator independently, all quadrature combinations (X_\pm^s, X_\pm^i) , (X_\pm^s, Y_\pm^i) , (Y_\pm^s, X_\pm^i) , (Y_\pm^s, Y_\pm^i) , can be measured for each setting of the polarization analyzers. Then, the homodyne detection data can be processed to compute the symmetrically ordered intensity correlations from

$$\langle I_\pm^s(\theta) I_\pm^i(\phi) \rangle_s = \langle [(X_\pm^s)^2 + (Y_\pm^s)^2][(X_\pm^i)^2 + (Y_\pm^i)^2] \rangle. \quad (29)$$

A recent measurement of the CHSH inequality for continuous variables employed a homodyne detection scheme similar to the one described here [40].

VI. CONCLUSION

In conclusion, we analyzed Bell's inequality violation in two-photon polarization correlations under different operator ordering of the intensity correlation functions. Under the usual experimental condition of weak parametric coupling (thin crystal), the normally ordered intensity correlations violate the CHSH criterion, while the symmetrically ordered ones do not. Beyond a technical issue, this operator ordering has a more profound physical meaning.

Normal ordering is imposed by photodetection signals based on photon absorption and therefore precludes any influence from the quantum vacuum, which energy cannot be extracted. Meanwhile, symmetric ordering is the usual prescription for constructing Hermitian operators from products of noncommuting observables. Moreover, symmetric ordering is crucial for evidencing vacuum effects like Casimir force, spontaneous emission, among many others [41]. The symmetrically ordered intensity correlations can be measured with the detection schemes discussed in Refs. [38,39]. We can also quote a recent measurement of the vacuum fluctuations, as reported in Ref. [42].

As a final remark, it is worthwhile to mention that for sufficiently large parametric interaction ($g\tau \sim 1$), no CHSH violation is predicted in either operator ordering. However, this regime falls outside the validity of the nondepletion assumption for the pump beam. In this case, the triple interaction between pump, signal, and idler must be fully solved, giving rise to triple correlations that may generate tripartite entanglement witnessed by other inequality criteria [43,44]. For example, strong parametric interaction is attained in four-wave mixing sources of entangled photon pairs [45–47]. The discussion drawn in this article will be pursued to the strong interaction regime in future contributions.

ACKNOWLEDGMENTS

Funding was provided by Conselho Nacional de Desenvolvimento Científico e Tecnológico (CNPq), Coordenação de Aperfeiçoamento de Pessoal de Nível Superior (CAPES), Fundação Carlos Chagas Filho de Amparo à Pesquisa do Estado do Rio de Janeiro (FAPERJ), and Instituto Nacional de Ciência e Tecnologia de Informação Quântica (INCT-IQ).

- [1] S. J. Freedman and J. F. Clauser, *Phys. Rev. Lett.* **28**, 938 (1972).
- [2] A. Aspect, P. Grangier, and G. Roger, *Phys. Rev. Lett.* **47**, 460 (1981).
- [3] J. S. Bell and A. Aspect, *Speakable and Unspeakable in Quantum Mechanics: Collected Papers on Quantum Philosophy*, 2nd ed. (Cambridge University Press, Cambridge, 2004).
- [4] P. G. Kwiat, A. M. Steinberg, and R. Y. Chiao, *Phys. Rev. A* **47**, R2472 (1993).
- [5] P. G. Kwiat, P. H. Eberhard, A. M. Steinberg, and R. Y. Chiao, *Phys. Rev. A* **49**, 3209 (1994).
- [6] G. Weihs, T. Jennewein, C. Simon, H. Weinfurter, and A. Zeilinger, *Phys. Rev. Lett.* **81**, 5039 (1998).
- [7] M. D. H. W. J. W. Pan, D. Bouwmeester and A. Zeilinger, *Nature (London)* **403**, 515 (2000).
- [8] G. Björk, P. Jonsson, and L. L. Sánchez Soto, *Phys. Rev. A* **64**, 042106 (2001).
- [9] G. B. M. B. Y. Hasegawa, R. Loidl and H. Rauch, *Nature (London)* **425**, 45 (2003).
- [10] D. N. Matsukevich, P. Maunz, D. L. Moehring, S. Olmschenk, and C. Monroe, *Phys. Rev. Lett.* **100**, 150404 (2008).
- [11] C. V. S. Borges, M. Hor-Meyll, J. A. O. Huguenin, and A. Z. Khoury, *Phys. Rev. A* **82**, 033833 (2010).
- [12] C. V. S. Borges, A. Z. Khoury, S. Walborn, P. H. S. Ribeiro, P. Milman, and A. Keller, *Phys. Rev. A* **86**, 052107 (2012).
- [13] L. J. Pereira, A. Z. Khoury, and K. Dechoum, *Phys. Rev. A* **90**, 053842 (2014).
- [14] B. Stoklasa, L. Motka, J. Rehacek, Z. Hradil, L. L. Sánchez-Soto, and G. S. Agarwal, *New J. Phys.* **17**, 113046 (2015).
- [15] W. F. Balthazar, C. E. R. Souza, D. P. Caetano, E. F. Galvão, J. A. O. Huguenin, and A. Z. Khoury, *Opt. Lett.* **41**, 5797 (2016).
- [16] D. Rauch, J. Handsteiner, A. Hochrainer, J. Gallicchio, A. S. Friedman, C. Leung, B. Liu, L. Bulla, S. Ecker, F. Steinlechner *et al.*, *Phys. Rev. Lett.* **121**, 080403 (2018).
- [17] J. F. Clauser, M. A. Horne, A. Shimony, and R. A. Holt, *Phys. Rev. Lett.* **23**, 880 (1969).
- [18] R. Loudon, *The Quantum Theory of Light* (Clarendon, Oxford, 1973).
- [19] L. Mandel and E. Wolf, *Optical Coherence and Quantum Optics* (Cambridge University Press, Cambridge, 1995).
- [20] J. Dalibard, J. Dupont-Roc, and C. Cohen-Tannoudji, *J. Phys. France* **43**, 1617 (1982).
- [21] S. De Bièvre, D. B. Horoshko, G. Patera, and M. I. Kolobov, *Phys. Rev. Lett.* **122**, 080402 (2019).
- [22] A. Casado, T. W. Marshall, and E. Santos, *J. Opt. Soc. Am. B* **15**, 1572 (1998).
- [23] M. Olsen, K. Dechoum, and L. Plimak, *Optics Commun.* **190**, 261 (2001).
- [24] L. F. da Silva, A. Z. Khoury, and K. Dechoum, *Phys. Rev. A* **78**, 025803 (2008).
- [25] A. Casado, S. Guerra, and J. Plácido, *Atoms* **7**, 76 (2019).
- [26] J. Eberly, *Contemp. Phys.* **56**, 407 (2015).
- [27] J. H. Eberly, X. F. Qian, A. Asma Al Qasimi, H. Ali, M. A. Alonso, R. Gutiérrez-Cuevas, B. J. Little, J. C. Howell, T. Malhotra, and A. N. Vamivakas, *Phys. Scr.* **91**, 063003 (2016).
- [28] X. F. Qian, T. Malhotra, A. N. Vamivakas, and J. H. Eberly, *Phys. Rev. Lett.* **117**, 153901 (2016).
- [29] J. H. Eberly, X.-F. Qian, and A. N. Vamivakas, *Optica* **4**, 1113 (2017).
- [30] F. D. Zela, *Optica* **5**, 243 (2018).
- [31] J. Gonzales, P. Sánchez, D. Barberena, Y. Yugra, R. Caballero, and F. D. Zela, *J. Phys. B: At. Mol. Opt. Phys.* **51**, 045401 (2018).
- [32] P. G. Kwiat, K. Mattle, H. Weinfurter, A. Zeilinger, A. V. Sergienko, and Y. Shih, *Phys. Rev. Lett.* **75**, 4337 (1995).
- [33] M. Franca Santos, P. Milman, A. Z. Khoury, and P. H. Souto Ribeiro, *Phys. Rev. A* **64**, 023804 (2001).
- [34] D. P. Caetano, P. H. Souto Ribeiro, J. T. C. Pardal, and A. Z. Khoury, *Phys. Rev. A* **68**, 023805 (2003).
- [35] H. Carmichael, *Statistical Methods in Quantum Optics 1* (Springer, Berlin, 1999).
- [36] M. V. I. Dononov, *Theory of Nonclassical States of Light* (Taylor and Francis, London, 2003).
- [37] K. Dechoum, M. D. Hahn, R. O. Vallejos, and A. Z. Khoury, *Phys. Rev. A* **81**, 043834 (2010).
- [38] B. Stiller, U. Seyfarth, and G. Leuchs, *Les Houches 2013: Quantum Optics and Nanophotonics (Chapter 4)* (Oxford University Press, Oxford, UK, 2017).
- [39] B. Stiller, U. Seyfarth, and G. Leuchs, [arXiv:1411.3765](https://arxiv.org/abs/1411.3765).
- [40] O. Thearle, J. Janousek, S. Armstrong, S. Hosseini, M. Schünemann (Mraz), S. Assad, T. Symul, M. R. James, E. Huntington, T. C. Ralph *et al.*, *Phys. Rev. Lett.* **120**, 040406 (2018).
- [41] P. Milonni, *The Quantum Vacuum. An Introduction to Quantum Electrodynamics* (Academic, Cambridge, MA, 1994).
- [42] I. C. Benea-Chelms, F. F. Settembrini, G. Scalari, and J. Faist, *Nature (London)* **568**, 202 (2019).
- [43] K. N. Cassemiro, A. S. Villar, M. Martinelli, and P. Nussenzveig, *Opt. Express* **15**, 18236 (2007).
- [44] A. S. Coelho, F. A. S. Barbosa, K. N. Cassemiro, A. S. Villar, M. Martinelli, and P. Nussenzveig, *Science* **326**, 823 (2009).
- [45] C. F. McCormick, A. M. Marino, V. Boyer, and P. D. Lett, *Phys. Rev. A* **78**, 043816 (2008).
- [46] V. Boyer, A. M. Marino, R. C. Pooser, and P. D. Lett, *Science* **321**, 544 (2008).
- [47] J. Ferraz, D. Felinto, L. H. Acioli, and S. S. Vianna, *Opt. Lett.* **30**, 1876 (2005).